A Himalayan-Scale Orogen in the Central African Copperbelt and the Formation of a World-Class Metal Province.

Tobermory Mackay-Champion *[1]

[1]Department of Earth Sciences, University of Oxford, South Parks Road, Oxford, UK.

Abstract The Central African Copperbelt (CACB) of Zambia and the Democratic Republic of the Congo is the world's largest sediment-hosted copper-cobalt province. It comprises Tonian–Ediacaran sedimentary rocks of the Katangan Basin and Ediacaran–Cambrian metamorphic and intrusive rocks formed during the assembly of Gondwana. The age distribution of metal deposits within the CACB peaks during the orogeny, indicating a significant orogenic control on mineralization. This study synthesizes existing structural, petrological, geochronological, and geophysical data to propose a new geodynamic model that reinterprets the CACB as a Himalayan-scale, continental-collision orogenic system. Its tectonic evolution is characteristic of a typical Wilson Cycle: continental rifting and ocean basin formation (∼880–650 Ma); oceanic subduction and pre-collisional metamorphism ($\leq$ 650 Ma); continent-continent collision ($\leq$ 570 Ma), leading to significant crustal thickening with burial depths reaching up to 45 km (∼530 Ma); and late-stage thrusting and magmatism ($\leq$ 510 Ma). The new model indicates that the CACB benefitted from two principal metal sources: metals derived from basement erosion, and metals introduced by magmatism during and after continent–continent collision, which is newly identified in this study. The next generation of metal deposits in the CACB will be found by locating outcropping or shallow subsurface magmatic intrusions.

1 Introduction

Sediment-hosted copper (Cu) deposits–comprising disseminated and veinlet Cu-sulfides within sedimentary rocks–currently account for ∼23 % of global copper production (Hammarstrom et al., 2019). These deposits are particularly attractive due to their relatively high grades and substantial ore volumes compared to porphyry Cu and volcanogenic massive sulfide (VMS) deposits, respectively (Dominish et al., 2019). However, exploration for sediment-hosted metal deposits has generally been less successful than for magmatic systems, largely due to an incomplete understanding of the first-order tectonic controls governing their distribution (Hoggard et al., 2020).

This challenge is exemplified by the Central African Copperbelt (CACB) of Zambia and the Democratic Republic of the Congo. The CACB is the world's largest sediment-hosted copper and cobalt province and contributes ∼14 %

*Corresponding author: tmackaychampion@gmail.com

and ∼60 % of the world's supply of these two metals, respectively (Selley et al., 2005). The CACB comprises Tonian–Ediacaran sedimentary rocks of the Katangan Basin and Ediacaran–Cambrian metamorphic and intrusive rocks. These rock assemblages formed through a sequence of continental rifting followed by basin closure and continent-continent collision between the Congo and Kalahari Cratons during the assembly of Gondwana (Porada and Berhorst, 2000). Research efforts have primarily focused on constraining the extensional history of the Katangan Basin, often under the assumption that mineralization is predominantly syn-diagenetic (Hitzman and Broughton, 2017). However, the age distribution of metal deposits peaks during the assembly of Gondwana, indicating a significant orogenic control on mineralization (Sillitoe et al., 2017). Despite this, no detailed geodynamic model exists for the CACB during this period. Interpretations of the CACB have largely emphasized a sedimentary-basin framework, with comparatively little focus on its orogenic evolution. Without this whole-system perspective, fundamental controls on the mineral system—including thermal gradients, fluid pathways, source rocks, metal traps, and crustal architecture—remain poorly understood. The CACB is estimated to contain ∼170 Mt of undiscovered copper resources (Hammarstrom et al., 2019), but exploration is significantly hampered by this knowledge gap (McCuaig and Hronsky, 2014).

In this study, I present a meta-analysis of existing structural, petrological, geochronological, and geophysical data to develop a new geodynamic model for the evolution of the CACB. I demonstrate that the CACB can be more accurately understood within an orogenic framework rather than through the traditional sedimentary-basin perspective. It exhibits striking similarities to classic collisional orogenic belts such as the Himalaya-Karakoram and the Scottish Caledonides, including regional metamorphism up to kyanite-grade conditions as well as a comparable tectonic configuration. The new model also offers an improved understanding of the mineral systems governing the CACB, particularly highlighting the potential role of magmatism-driven mineralization. In Section 2, I outline the large-scale tectonic setting of the CACB. Section 3 presents a reinterpretation of the geological characteristics of individual domains within the CACB orogenic system, revealing a previously unrecognised tectonic framework. The new geodynamic model is introduced in Section 4, followed in Section 5 by an analysis of the CACB mineral system within this new framework. Despite differences in erosion levels among orogens of varying ages, there are clear similarities in their overall structural architecture, metamorphic conditions, and geochronological evolution (Weller et al., 2021). Accordingly, comparisons with analogous orogenic systems are drawn where relevant to enhance understanding of the CACB.

2 Geological setting of the CACB

The geological evolution of the CACB and its surrounding regions can be broadly categorized into four major time periods and associated litho-tectonic assemblages (Figure 1): (1) the Archaean and Palaeoproterozoic Congo, Bangweulu, and Kalahari cratons, which crop out to the northwest, northeast, and south of the CACB respectively. These terranes exhibit lithospheric thicknesses in excess of 200 km (Schaeffer and Lebedev, 2013). (2) the Mesoproterozoic Irumide and Kibaran belts, which formed part of the Central African Shield during the assembly of Rodinia (Villeneuve et al., 2023), (3) the Katangan Basin, which formed as a result of extension and subsequent rifting between the Congo and Kalahari cratons during the Neoproterozoic (Purkiss, 2025; Daly et al., 2025) and, (4) the < 650 Ma Lufilian Orogen, comprising rocks up to kyanite-grade metamorphic conditions and high levels of deformation (Porada and

Berhorst, 2000). The orogen formed as a result of basin closure and orogenesis associated with continent-continent collision and the assembly of Gondwana. This study uses the term CACB to refer to both the Katangan Basin and the Lufilian Orogen, reflecting their temporal and structural continuity as well as the presence of metal deposits in both regions.

3 Tectonic domains of the CACB

The CACB can be viewed as an approximately north-to-south progression from the Congo Craton through: (1) the Katangan Basin, (2) the External Fold-Thrust Belt, (3) the Domes Region, (4) the Synclinorial Belt, (5) the Lufilian Suture Zone (comprising the Katanga High and Zambezi Belt), and finally the Kalahari Craton (Figure 1). In contrast to the traditional view, the Katanga High and Zambezi Belt are treated here as a single composite domain based on their metamorphic, structural, and geochronological continuity (Figure 1; see Section 3.5). The following sub-sections discuss the structural, metamorphic, and geochronological characteristics of each domain.

3.1 Katangan Basin

This region is characterized by sub-horizontal to gently dipping Katangan Supergroup sedimentary rocks onlapping Congo, Kibaran, Bangweulu, and Irumide basement rocks (Daly et al., 2025). This represents an autochthonous remnant of the Katangan Basin, which formed as a result of two-stage rifting between the Congo craton to the north and the Kalahari craton to the south (present day coordinates) over a protracted ~300 Myr timeframe (Purkiss, 2025; Daly et al., 2025): The first stage of rifting began sometime after ~880 Ma during the Tonian Period, resulting in the deposition of syn-rift Lower Roan Group sedimentary rocks. Above it, the Upper Roan Group marks a transition to post-rift conditions, representing shallow marine and coastal environments formed during thermal subsidence. The Mwashia Group reflects a second period of rifting and associated magmatic activity commencing at ~765 Ma, with deepening of the basin characterised by marine flooding surfaces (Purkiss, 2025). The northwest and southeast margins of the basin comprise fault-controlled subbasins with extensive Mwashia-age extrusive and intrusive mafic units (Kampunzu et al., 2000). Above the Mwashia lies the Nguba Group, which spans the Sturtian glaciation and represents a deep, often sediment-restricted basin bounded by a maximum flooding surface. Finally, the Kundelungu Group was deposited from the beginning of the Ediacaran period and represents a distal, quiet basin (Purkiss, 2025). This culminates in the Plateau Group, interpreted as a continental molasse (Wendorff, 2005). Historically referred to as the Shaba, Katangan or Kundulungu aulacogen or Golfe du Katanga (De Swardt et al., 1964; Porada and Berhorst, 2000), this northern region has previously been recognized as the stable foreland of the CACB (e.g., Wendorff, 2005). The hydrothermal, vein-hosted copper deposits of Dikulushi, Safari, and Shaba are found here (Taylor et al., 2013; Padilla et al., 2021).

3.2 External Fold-Thrust Belt

Structurally above the foreland succession lies the External Fold-Thrust Belt, which crops out along the Zambia–DRC border and the southern DRC. This domain contains the highest number of known metal deposits, including mines such as Konkola with reserves of $\geq$140.3 Mt Cu. The belt is characterized by northward-directed thin-skinned thrusting and imbrication of Katangan Supergroup sedimentary rocks and their low-grade metamorphic equivalents

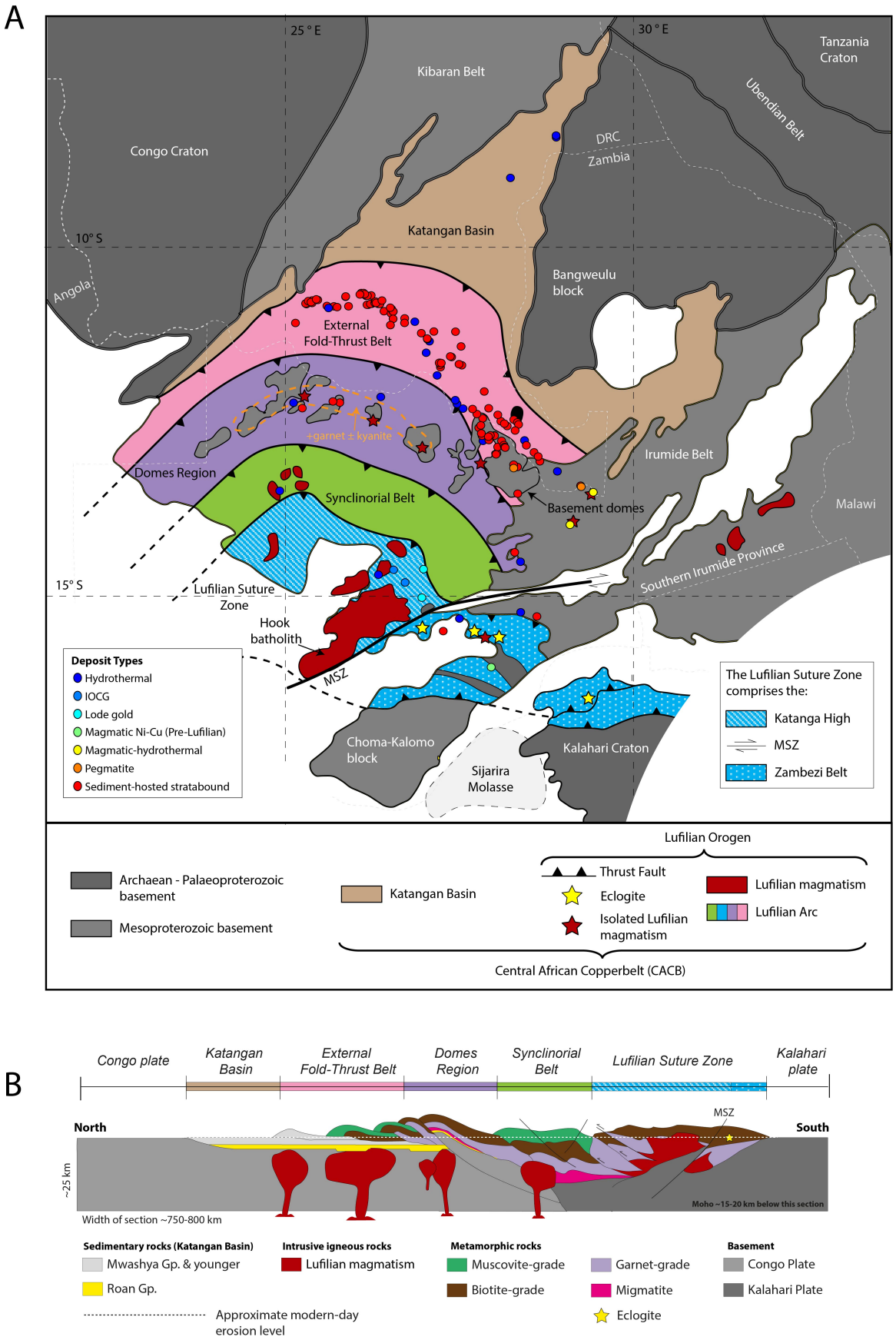

Figure 1 A) Tectonic map of the Central African Copperbelt modified after Eglinger et al. (2013) and Daly et al. (2025). The newly defined *Lufilian Suture Zone* has been divided into the north-western Katanga High and the south-eastern Zambezi Belt, separated by the Mwembeshi Shear Zone (MSZ). These terranes are combined due to their metamorphic, structural, and igneous continuity during the Lufilian orogeny (Section 3.5). The mine locations and deposit types are taken from Taylor et al. (2013) and Padilla et al. (2021). B) Schematic cross-section of the Central African Copperbelt. *N.B. the Lufilian magmatism is not to scale*.

above evaporite-rich detachments (Coward and Daly, 1984). These detachments accommodated significant lateral transport of up to 65–150 km northwards (Porada and Berhorst, 2000; Jackson et al., 2003). The evaporites also facilitated fluid overpressuring and diapirism, as well as the extrusion of salt glaciers (Jackson et al., 2003). The metamorphic grade of the external belt decreases from greenschist to prehnite-pumpellyite down structural section towards the north (Selley et al., 2005). The belt hosts Lufilian-age pegmatites associated with emerald mineralization and magmatic-hydrothermal deposits aged between 530–517 Ma (Perelló et al., 2022; Seifert et al., 2004). Along strike to the south-east, the Southern Irumide Belt contains granites and syenites emplaced between 534–465 Ma (Johnson et al., 2006). These intrusions likely represent magmatic bodies emplaced into the footwall of the External Fold-Thrust Belt, now exposed as a result of extensive erosion and Cenozoic rifting. These intrusions are coeval with high-pressure metamorphism in the Chewore-Rufunsa terrane of the Southern Irumide Belt (Johnson et al., 2006). Metamorphic monazite ages in the fold-thrust belt cluster around 530 Ma, while Ar–Ar biotite cooling ages cluster between 490–475 Ma (Rainaud et al., 2005) (Figure 3). This reflects peak metamorphism followed by post-tectonic uplift and cooling.

3.3 Domes Region

Structurally above the fold-thrust belt lies the Domes Region, named after five antiformal domes of Mesoproterozoic basement rock that crop out along strike from one another in northwest Zambia. The Domes Region is an arcuate zone approximately 50 km across strike and represents the deepest structural levels and highest metamorphic grades of the entire CACB. Based on these observations, the Domes Region has previously been interpreted as the locus of maximum shortening during the Katangan Basin inversion (Goscombe et al., 2020; Daly et al., 2025). The metasedimentary rocks in the Domes Region range from biotite to garnet-kyanite grade, with local evidence for partial melting (Cosi et al., 1992; John et al., 2004; Eglinger et al., 2016). Peak metamorphic pressures of 13 kbar (∼45 km burial) indicate substantial crustal shortening and thickening. These metamorphic rocks can now be found in thrust contact with undeformed, unmetamorphosed Katangan sedimentary rocks in underlying half-grabens (Daly et al., 2025). This requires substantial lateral transport from their site of metamorphism—consistent with the large displacements seen in the External Fold-Thrust Belt.

Peak metamorphic conditions in the Domes Region were achieved at ∼530 Ma (monazite–John et al., 2004; garnet–Eglinger et al., 2016). The region hosts significant mineralization, including Kansanshi and Sentinel with resources of 1,125.4 Mt and 648.7 Mt Cu respectively, as well as the Enterprise hydrothermal nickel mine (Capistrant et al., 2015). The Domes Region also hosts Lufilian-age pegmatites (∼ 530 Ma; Selley et al., 2018) and late-Cambrian alkali granites and nepheline syenites (Cosi et al., 1992). These intrusions likely correspond to granitic bodies inferred beneath the northern CACB from magnetic anomaly data (Selley et al., 2018). Supporting this interpretation, regional gravity data indicate that the Domes Region exhibits anomalously low mass, consistent with substantial volumes of low-density granitic material at depth (Selley et al., 2018).

3.4 Synclinorial Belt

South of the Domes Region lies the Synclinorial Belt, composed of intensely deformed rocks ranging from argillaceous sedimentary rocks to biotite-grade metapelites (Porada and Berhorst, 2000; Goscombe et al., 2020). It features

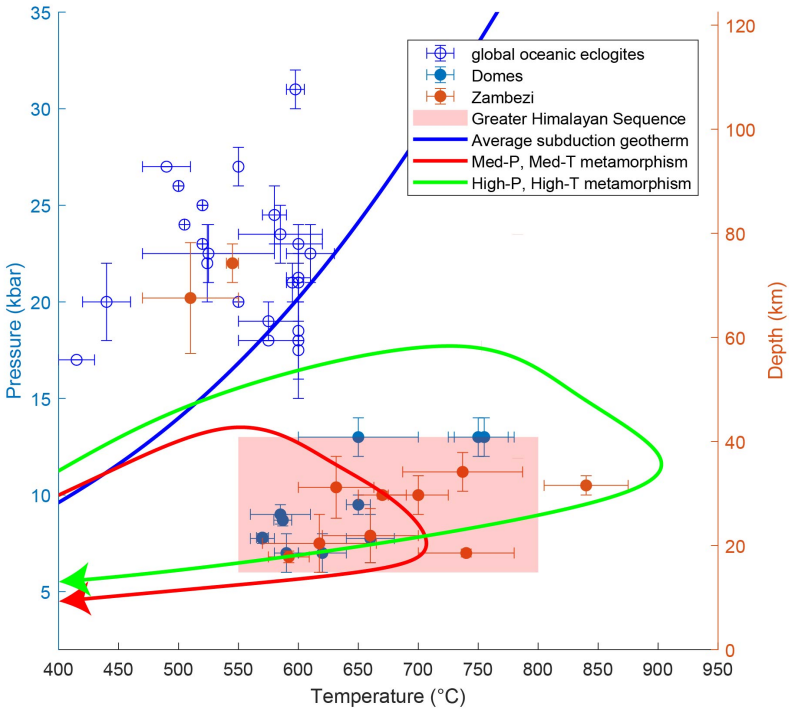

Figure 2 Pressure-temperature conditions experienced by the Domes Region and Zambezi Belt of the Lufilian Suture Zone. The Greater Himalayan Sequence conditions were taken from Waters (2019). The compilation of global oceanic eclogites from Chen et al. (2013), and the Barrovian P-T paths from Weller et al. (2021). The high pressures recorded in the CACB necessitate significant crustal thickening.

steep, north-vergent folds and shows little evidence of salt tectonics (Daly et al., 2025). This domain remains relatively understudied, due to limited outcrop and the lack of active mining operations.

3.5 Lufilian Suture Zone

Structurally overlying the Synclinorial Belt is the newly defined Lufilian Suture Zone, comprising the Katanga High, Hook Batholith, Mwembeshi Shear Zone, and Zambezi Belt. This unification of previously distinct lithotectonic assemblages is based on a revised interpretation of the Mwembeshi Shear Zone, outlined below.

3.5.1 The Mwembeshi Shear Zone

The south-eastern margin of the CACB has typically been defined by the Mwembeshi Shear Zone (MSZ) (e.g., De Swardt et al., 1964), although its tectonic significance is debated. Some regard the MSZ as a suture zone between the Congo and Kalahari cratons (e.g., Coward and Daly, 1984; Daly et al., 2025). However, no change in shear-wave anisotropy or crustal thickness is observed across the MSZ (Kounoudis et al., 2024; Ogden et al., 2025). Sedimentary successions can be traced into the northern part of the Zambezi Belt from the southern Katanga High (Porada and Berhorst, 2000), and there is a continuity of kyanite-grade metamorphism and structures between the northern part of the Zambezi Belt and the Matala Dome, which lie on opposing sides of the MSZ (Naydenov et al., 2016; Simpson, 1962). These observations suggest that the MSZ is not a lithospheric-scale structure contrasting significantly distinct geological terranes (Naydenov et al., 2014). Consequently, the MSZ may be better interpreted as a minimal-offset fault that divides the otherwise continuous Katanga High, Hook Batholith, and Zambezi Belt. These regions are therefore more appropriately regarded as components of a unified Lufilian Suture Zone.

3.5.2 The Katanga High and the Hook Batholith

The Katanga High comprises extensive outcrops of carbonate rocks and low- to kyanite-grade metapelites, with north–south–trending folds cross-cut in the north by an east-northeast to west-southwest fold belt (De Swardt et al., 1964; Naydenov et al., 2016). The region also contains the Matala Dome, a basement inlier surrounded by kyanite-grade metasedimentary rocks (Naydenov et al., 2016).

The south-east section of the Katanga High is intruded by the Hook Batholith, a syn-tectonic, 570—530 Ma, bi-modal magmatic body (Hanson et al., 1993; Milani et al., 2015; Naydenov et al., 2014). The batholith predominantly crops out in south-west Zambia, but can also be found in the Zambezi Belt (Hanson et al., 1988). The felsic units consist of an alkali-calcic suite of monzogranite, granodiorite and granite and an alkali suite of syenite and alkali-granite (Naydenov et al., 2014). High primary water contents in the Hook Batholith are indicated by the abundance of primary amphibole (Naydenov et al., 2014). The metaluminous geochemistry and Sr–Nd isotopic signatures, which overlap with those of ocean-island basalts, rule out derivation from a purely sedimentary protolith and instead point to significant contributions from mantle-lithologies. This is supported by the presence of syn-tectonic gabbroic intrusions (Milani et al., 2015) and underpins the hypothesis that the Hook Batholith began forming above a subducting slab, where mantle-derived melts intruded and triggered partial melting of the overlying crust (Milani et al., 2015; Naydenov et al., 2014). The Hook Batholith hosts a number of Cu deposits, some with iron oxide-copper-gold (IOCG) characteristics (Milani et al., 2019).

3.5.3 The Zambezi Belt

To the southeast of the MSZ lies the Zambezi Belt of southern Zambia and northern Zimbabwe. The Zambezi belt comprises the Zambezi Supercrustal Sequence (ZSC) and inliers of Mesoproterozoic gneissic and granitoid basement (Hanson et al., 1988). The ZSC is a sequence of Neoproterozoic sedimentary, volcanic and volcaniclastic rocks that have been variably metamorphosed up to upper amphibolite-facies conditions (Johnson et al., 2007). The protoliths of the ZSC are interpreted to be the correlatives of the lower units of the Katangan Supergroup (De Swardt et al., 1964; Johnson et al., 2007). The Zambezi Belt lies upon a Mesoproterozoic granitic basement including the ∼1106 Ma Mpande Gneiss and the ∼1090 Ma Munali Hills Granite (Hanson et al., 1988; Katongo et al., 2004). Extension in the Zambezi Belt began at ∼880 Ma, with the basement unconformably overlain by a series of bimodal metavolcanic rocks and phyllites known as the Kafue Rhyolite Formation and the Nazingwe Formation, respectively (Hanson et al., 1993; Johnson et al., 2007). This was coeval with the onset of extension in the Katangan Basin, as constrained by the 883 ± 10 Ma age of the Nchanga Granite (Armstrong et al., 2005). Continued extension saw the intrusion of the ∼820 Ma Ngoma Gneiss, and other magmatic bodies such as the Munali ultramafic body, which hosts a magmatic sulfide nickel deposit (Holwell et al., 2017). A second phase of magmatism occurred between 764–737 Ma, preserved in the Makuti Group felsic extrusives of the Central Zambezi Belt (Dirks et al., 1999), which overlaps with the Mwashia-age rifting event and accompanying magmatism in the Katangan Basin (Purkiss, 2025).

During the assembly of Gondwana, the Zambezi Belt experienced significant NE–SW shortening, developing a steep, bivergent flower structure that exhumed reworked basement thrust slices and emplaced allochthonous nappes above the northern margin of the Kalahari Craton (Johnson et al., 2007). The uppermost section of the ZSC hosts

numerous peridotitic, gabbroic, and metagabbroic bodies with N-MORB signatures, interpreted as a dismembered ophiolite sequence (John et al., 2003; Johnson et al., 2005). These bodies occur in close association with eclogites interpreted to have formed in an oceanic subduction-zone setting. These eclogites are dated between 659 ± 14 Ma and 595 ± 10 Ma (Vrána et al., 1975; Johnson et al., 2005; John et al., 2003), and record peak prograde conditions of 540–550 °C at 21.0–23.0 kbar (Chombwa locality) and 470–550 °C at 17.8–23.0 kbar (Lusaka locality) (Goscombe et al., 2020). Contemporaneous with eclogite formation, rocks of the Zambezi Belt experienced amphibolite-facies metamorphism and monazite growth at 650–630 Ma, indicative of metamorphism along the Kalahari Craton margin prior to continent–continent collision (Sakuwaha et al., 2022). This is followed by a pronounced cluster of metamorphic monazite ages between 570–530 Ma, corresponding to metamorphic conditions of 10–12 kbar (Johnson et al., 2005; Goscombe et al., 2020; Sakuwaha et al., 2022; **?**; Kuribara et al., 2019). This is coeval with peak metamorphism in the Domes Region, with both the Domes Region and the Zambezi Belt attaining comparable peak metamorphic conditions (Figure 2).

3.6 Southern margin

The Kalahari Craton, exposed to the south of the CACB, comprises the Archean Zimbabwe and Kaapvaal cratons and grew by prolonged crustal accretion in the Palaeoproterozoic-Mesoproterzoic, amalgamating terranes such as the Choma–Kalomo Block, the Chewore Terrane and the Kaourera Terrane (Goscombe et al., 2020). The overyling Sijarira Group molasse contains 570 Ma to ∼515 Ma detrital zircons, and can be correlated with the Kundelungu Group on the northern foreland (Foster and Goscombe, 2013).

4 Tectonic Synthesis

4.1 Similarities to other orogens

The CACB exhibits many characteristics common to well-documented collisional orogens, in particular the spatial-temporal succession of lithologic assemblages and superimposed tectonothermal events (Figure 3). South of the Congo Craton and the undeformed foreland sedimentary rocks of the Katangan Basin, the External Fold–Thrust Belt of the Lufilian Orogen is characterized by low-grade metamorphism and pervasive thrust deformation. This resembles foreland systems such as the deformational front of the Appalachian-Caledonide system (negligible to low-grade metamorphism) and the Lesser Himalaya (typically greenschist facies) (Searle, 2022). However, the concentration of strain above salt-rich detachments is more akin to that in the Southern Pyrenees (e.g., Cámara and Flinch, 2017) and the Salt Range of Pakistan (e.g., Ghazi et al., 2015).

Progressing structurally upward and into the hinterland, the Domes Region records a markedly higher metamorphic grade, with both right-way-up and inverted metamorphic sequences progressing from biotite- to kyanite-grade conditions (Ridgway and Ramsay, 1986) and locally attaining partial melting—a typical Barrovian-type sequence. This architecture mirrors that of the Greater Himalayan Sequence and the Moine metamorphic rocks of the Scottish Caledonides (Searle, 2022). The pressure–temperature (P–T) conditions recorded in the Domes Region range from 550–800 °C and 6–13 kbar, closely matching those observed in the Greater Himalayan Sequence of the Himalayan orogen (Waters, 2019) (Figure 2). These pressures correspond to burial depths of approximately 45 km—far beyond what can be achieved through sedimentary loading—and instead require substantial crustal shortening and thickening

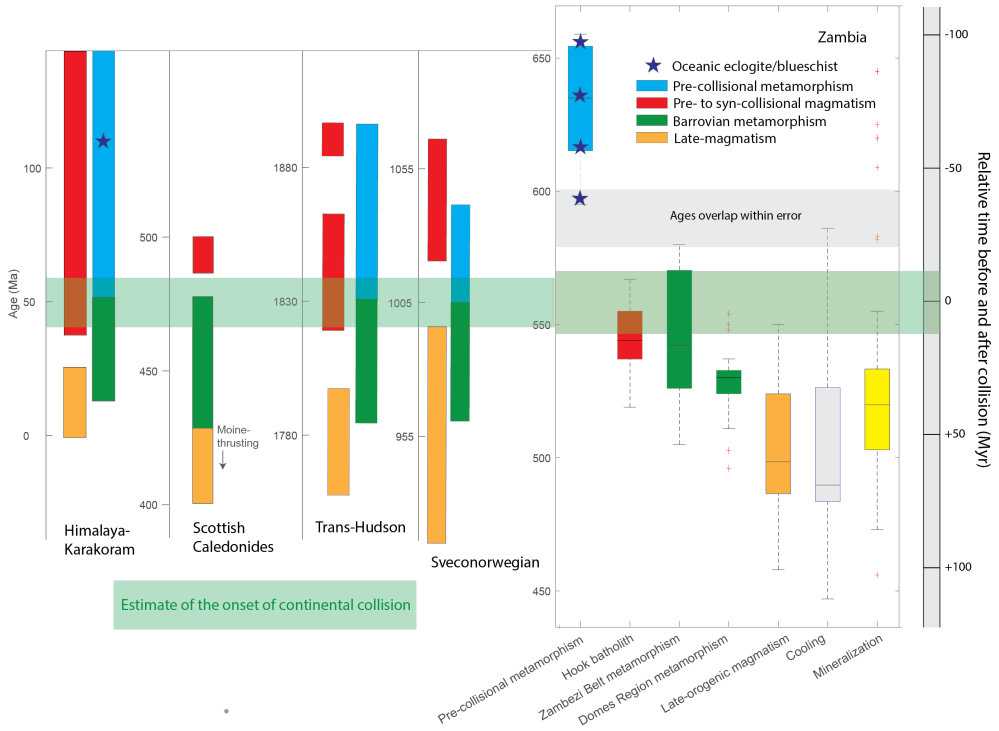

Figure 3 Geochronological comparison between the CACB and other Himalayan-scale orogens. The evolution of the Trans-Hudson and Sveconorwegian orogens are taken from Weller et al. (2021), the evolution of the Himalaya-Karakoram from St-Onge et al. (2006), and the evolution of Scottish Caledonides from Searle (2022).

associated with the collision between the Congo and Kalahari continental plates. Peak metamorphism occurred at ~ 530 Ma, coinciding with peak metamorphism in other regions involved in the assembly of Gondwana (Cawood and Buchan, 2007).

The Lufilian Suture Zone closely resembles the Tethyan Sequence and Indus-Tsangpo Suture Zone of the Himalaya: both exhibit epizonal- to amphibolite-grade metamorphism (Dunkl et al., 2011), contain dismembered ophiolitic fragments and subduction-related blueschist- to eclogite-facies rocks (John et al., 2003; O'Brien, 2019), and record foreland-directed thrusting that steepens and then overturns toward the hinterland (Corfield and Searle, 2000). Similar features are also seen in the suture zone of the Scottish Caledonides (Searle, 2022). The 650–595 Ma eclogites of the Zambezi Belt record metamorphic conditions equivalent to burial depths of up to 80 km and are fully consistent with those of oceanic eclogites worldwide (Figure 2), necessitating a phase of oceanic subduction prior to continent-continent collision (John et al., 2003). This is akin to the 100 Ma blueschists of Ladakh in the Himalayan orogen (O'Brien, 2019).

The Zambezi Belt preserves evidence of medium-temperature–medium-pressure metamorphism coeval with this period of oceanic subduction. Regional metamorphism prior to continent-continent collision is well documented in orogenic systems. For example, the Karakoram experienced amphibolite-grade metamorphism during the Cretaceous (Fraser et al., 2001). In the North American Cordillera, significant crustal thickening and high-grade metamorphism during the Laramide Orogeny were driven by flat-slab subduction in the Late Cretaceous to Paleocene, resulting from increased traction along the plate interface and enhanced end-loading at the trench (Yonkee and Weil, 2015). This mechanism has also been suggested for the Scottish Caledonides (Lamont et al., 2025). The Lufilian Suture Zone then experienced substantial crustal thickening up to 12 kbar during the subsequent continent-continent collision.

This began at 570 Ma and progressed through to 530 Ma, coinciding with peak metamorphism of comparable grade in the Domes Region.

The Hook Batholith is the only pre- to syn-collisional magmatism recorded in the CACB. The lack of pre-collisional calc-alkaline magmatic arc preserved in Zambia has caused confusion. It should be noted that well-known collisional zones which previously experienced oceanic subduction, such as the Alps, do not contain such an arc (McCarthy et al., 2018), and it is almost certain that any subduction-related magmatic arc would now underlay the Lufilian Suture Zone. The CACB also exhibits late-stage magmatism and thrusting, which overlap with and postdate peak crustal thickening. For example, syenites are observed cropping out in the Domes Region (Cosi et al., 1992) and granitic pegmatites are found in the External Fold-Thrust Belt (Seifert et al., 2004). These intrusions, aged between ~534–465 Ma, are contemporaneous with high-temperature metamorphism and granite magmatism documented in other parts of the Gondwana assembly (Cawood and Buchan, 2007). The intrusion of late-stage granites is analogous to the "Newer Granites" of the Scottish Caledonides (Pankhurst and Sutherland, 1982), as well as the 960-935 Ma granitic pegmatites in the Sveconorwegian orogen (Möller et al., 2007). Finally, to the north and south of the Lufilian Orogen lie the Plateau Group and Sijairi molasses, respectively. These are akin to the Siwalik molasse basin which formed along the southern margin of the Himalaya during the uplift of the mountain chain (St-Onge et al., 2006).

4.2 A new model for the CACB

The tectonic evolution of the CACB can be divided into several phases indicative of a typical Wilson Cycle. Figure 4 provides a schematic illustration of this evolution, beginning with the onset of subduction. The numbered stages in Figure 4 are referenced throughout the text as F4.1, ..., F4.N.

Continental extension (880–765 Ma) Extension between the Congo and Kalahari cratons began at a maximum of 880 Ma, as constrained by the age of the Nchanga granite which unconformably underlies the CACB (Armstrong et al., 2005). This extension provided accommodation space for the deposition of the Lower and Upper Roan Group sedimentary rocks in the CACB and the lowermost units of the Zambezi Supercrustal Group (F4.2)(Purkiss, 2025; Johnson et al., 2007; Daly et al., 2025). Minor igneous units were intruded during this time, including the Ngoma Gneiss and the Munali ultramafic body (Holwell et al., 2017).

Ocean basin formation (765–650 Ma) A second phase of rifting is preserved in the Mwashia Group of the CACB, during which there was extensive mafic magmatism (Purkiss, 2025). This period is interpreted to record the final stages of continental breakup and the formation of oceanic crust. The increase in mafic magmatism prior to final rifting is commonly observed in rift settings (e.g., Sun et al., 2019). The size of the resulting ocean basin is largely unconstrained (F4.1) but must have been relatively sizeable as the Congo and Kalahari craton margins become distinct entities with contrasting palaeomagnetic and detrital zircon records (Foster and Goscombe, 2013; Goscombe et al., 2020).

Oceanic subduction and pre-collisional metamorphism (650 Ma onwards) Oceanic subduction began sometime during the Cryogenian, evidenced by the ~650 Ma eclogites preserved in the Zambezi Belt of the Lufilian Suture Zone (F4.3) (John et al., 2004). Today, the eclogites are found in close relationship with oceanic metasedimentary

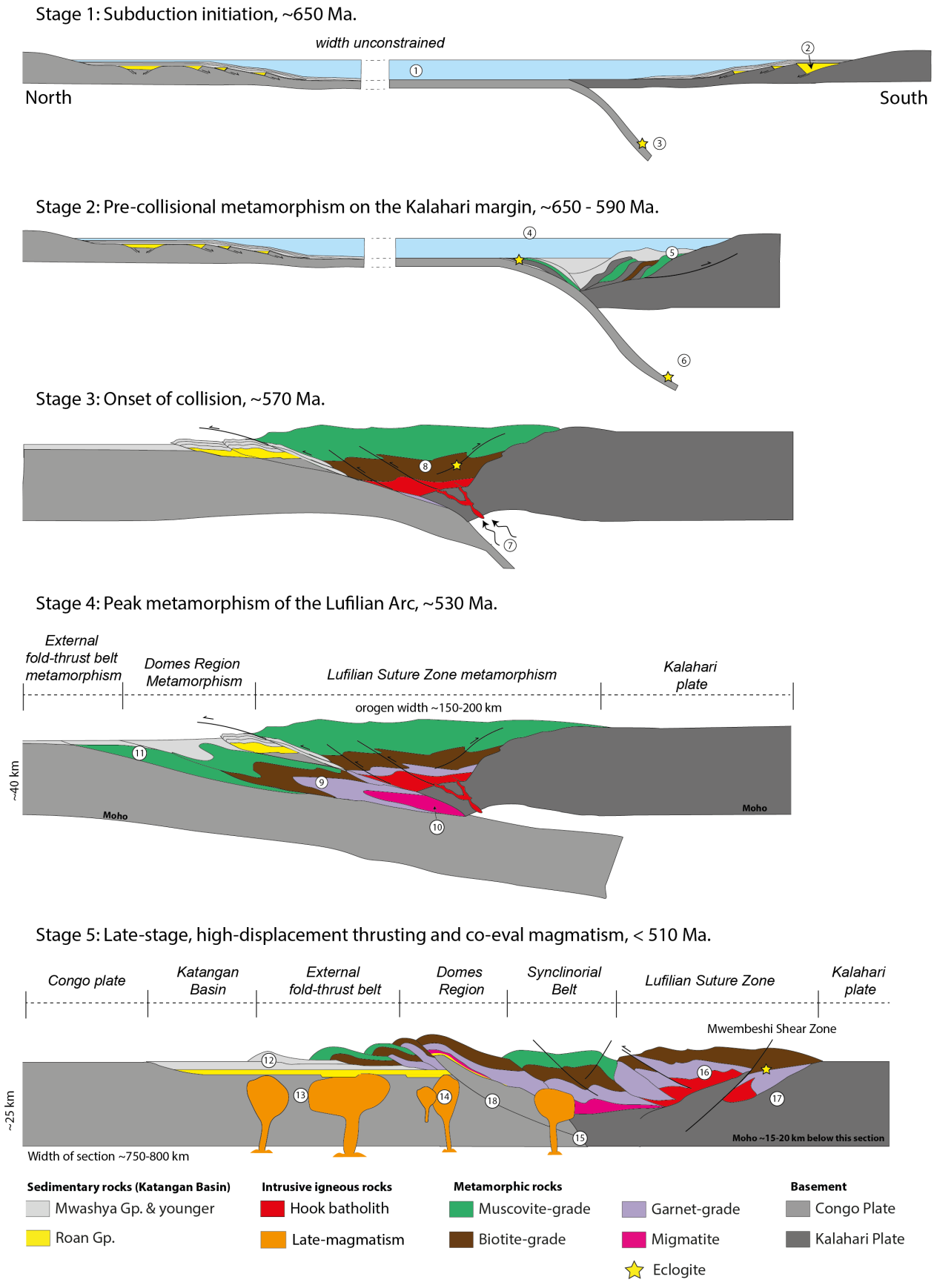

Figure 4 Tectonic model of the CACB.

rocks and ophiolitic fragments (F4.4). With metamorphic conditions of ∼540–550 °C and ∼21–23 kbar, these eclogites clearly preserve a subduction geotherm (John et al., 2003; Goscombe et al., 2020). Eclogite-facies metamorphism continued until 595 ± 10 Ma (John et al., 2003) (F4.6). Concurrent with oceanic subduction, the Kalahari Plate underwent medium-temperature/medium-pressure metamorphism at 570–665 °C and 6.5–9 kbar from 656±16 Ma-635±2 Ma (Fig. 4.5; Sakuwaha et al., 2022).

Onset of collision (∼570 Ma) The exact timing of collision is still a point of significant debate in well-preserved, modern orogens such as the Himalaya (Hu et al., 2016). Consequently, it is unlikely we will be able to resolve the exact timing of collision in the CACB. However, a new period of garnet-grade conditions and metamorphic monazite growth are recorded in the Zambezi Belt at ∼570 Ma (F4.8) (Johnson et al., 2007; Sakuwaha et al., 2022). The Hook Batholith magmatism also began at at this time as a result of crustal and mantle fluid-flux melting (Milani et al., 2015). These melts would have intruded the overlying metasedimentary rocks of the Lufilian Suture Zone and the Kalahari plate (F4.7).

Peak metamorphism (∼530 Ma) Peak metamorphic conditions in both the Domes Region and the Lufilian Suture Zone were attainted at ∼530 Ma (e.g., John et al., 2004; Eglinger et al., 2016; Naydenov et al., 2016). The Domes Region progressed into a significant orogenic wedge akin to the Greater Himalayan Sequence (F4.9). Metamorphic conditions reached kyanite-grade, with preserved evidence of partial melting (F4.10) (Eglinger et al., 2016). The External Fold-Thrust Belt experienced greenschist-facies metamorphism (F4.11) (Rainaud et al., 2005). The molasse of the Kundelungu (north) and the Sijarira Group (south) formed as the result of erosion during exhumation of the intervening orogenic core.

Late-thrusting and magmatism (< 510 Ma) Following peak metamorphism, the orogenic belt experienced significant lateral transport towards both the south and north. This is evidenced by the preservation of kyanite-grade metasedimentary rocks directly atop autochthonous undeformed sedimentary rocks in the Domes Region (Daly et al., 2025). The timing of this event is not well constrained but likely occurred at ∼510 Ma as evidenced by zircon overgrowths in the autochthonous lithologies (Barron, 2003). The most significant transport occurred in the External Fold-Thrust Belt, characterized by northward thin-skinned thrusting and imbrication of the Katangan Supergroup stratigraphy above evaporite-rich detachments (Coward and Daly, 1984). These lubricated detachments accommodated lateral transport of up to 65–150 km northwards (F4.12) (Porada and Berhorst, 2000; Jackson et al., 2003). These significant displacements and the curvilinear thrusting related to the syntaxial geometry of the orogen explain the significant across-strike width of the CACB, comparable to that observed in the western syntaxis of the Himalaya in Pakistan (e.g., Ghazi et al., 2015). The late-stage thrusting also involved thick-skinned, out-of-sequence exhumation of basement rocks in the Domes Region and the Zambezi Belt (Fig. 4.12). This is observed in the Moine Thrust Zone of the Scottish Caledonides, with out-of-sequence thrusting of basement Lewisian Gneiss over Cambro-Ordovician sedimentary rocks (e.g., Searle et al., 2019). Similar observations can be made in the fold-and-thrust belts of the Appalachian and Grenvillian orogenic fronts (van Gool et al., 2008).

Late-thrusting was coeval with the intrusion of granites and syenites (F4.13). Syenites are observed cropping out

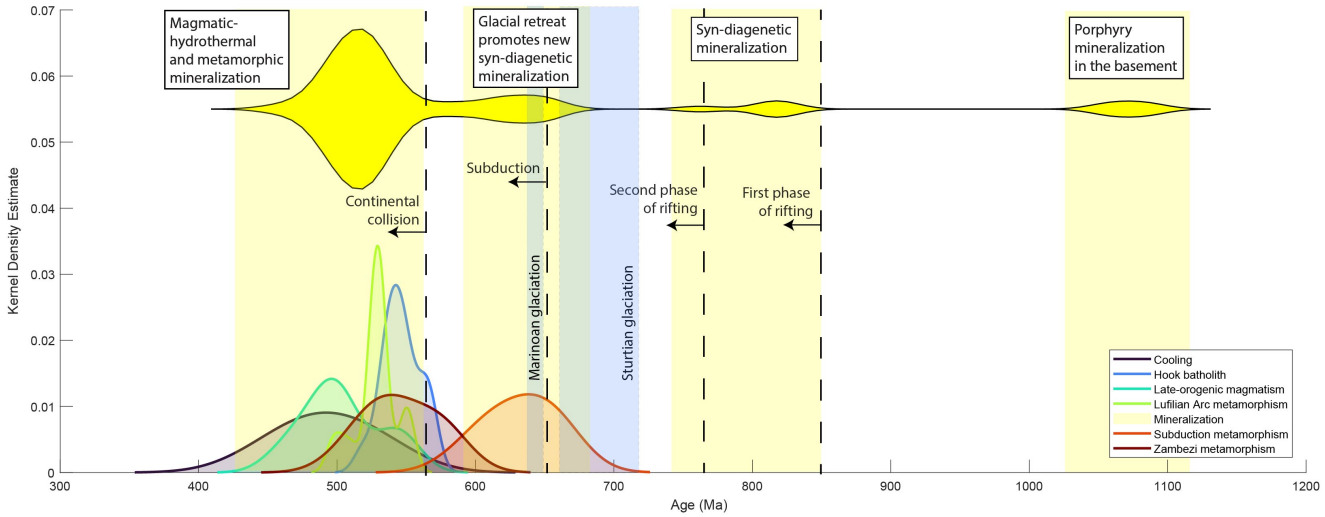

Figure 5 Mineralization and tectonothermal events in the CACB. The timing of the Snowball Earth glaciations were taken from Hoffman et al. (2017), the timing of the two rifting events was taken from Purkiss (2025).

in the Domes Region (Cosi et al., 1992) and into the Southern Irumide Belt (footwall of the CACB) between 534–465 Ma (Johnson et al., 2006). Lufilian-age granitic pegmatites are also found in the Domes Region (F4.14) (Selley et al., 2018) and the External Fold-Thrust Belt (Seifert et al., 2004). The observed change in the direction and magnitude of mantle anisotropy indicates that the Congo–Kalahari craton boundary now lies beneath the Synclinorial Belt (Kounoudis et al., 2024) (F4.15). The Mwombeshi Shear Zone is interpreted as a late, right-lateral, oblique-slip fault with a reverse component (F4.17), which has likely helped to exhume the Hook batholith. Late Lufilian-age IOCG, lode-gold and hydrothermal metal deposits are found neighbouring the Hook (F4.15) (Milani et al., 2015).

Post-orogenic uplift and cooling (< 500 Ma) The abundance of mica cooling ages indicates post-orogenic uplift began at ∼500 Ma. This is supported by zircon fission-track thermochronometry from sandstones in Solwezi (NW Zambia) which shows that uplift took place from 500–400 Ma (Daly et al., 2025). Granitoids continued to be intruded during this period (Johnson et al., 2006).

5 The mineral system of the CACB

A Kernel Density Estimation of geochronological ages from mineralized and coeval phases in deposits around the CACB was used to characterize the temporal distribution of mineralization and its relationship to tectonic events (Figure 5). This analysis demonstrates that there are four key periods of mineralization. Firstly, there is evidence of appreciable Mesoproterozoic mineralization in the basement of the CACB at 1084–1059 ± 5 Ma (Sillitoe et al., 2015; Master and Ndhlovu, 2019). This is thought to be the result of porphyry-systems active during the Irumide Orogeny (Rainaud et al., 2005), and is a key source of metals for the overlying Katangan Basin (Cailteux et al., 2005).

Secondly, there is evidence of syn-diagenetic mineralization of Katangan Supergroup sedimentary rocks within the External Fold-Thrust Belt. For example, the Kamoto deposit of the DRC contains mineralization dated at 821 ± 51 and 762 ± 33 Ma (Muchez et al., 2015). The “red-bed” model is currently the prevailing genetic framework for syn-diagenetic mineralization in the CACB (Hitzman et al., 2005). This model posits that metal deposits formed through the migration of oxidized, metal-rich basinal fluids into reduced lithologies—typically carbonaceous shales—during

sediment deposition and diagenesis. These metals are thought to originate from the chemical leaching of red-bed sedimentary sequences within the Katangan Basin. The KDE analysis indicates that syn-diagenetic deposits contribute only marginally to the CACB's metal budget by deposit count, challenging traditional interpretations.

Thirdly, there is evidence of a pulse of mineralization from ~ 652–609 Ma (Saintilan et al., 2018; Cahen, 1961; Decrée et al., 2011). Mineralization of this age is preserved across the Domes Region and External Fold-Thrust Belt, including Ndola (Cahen, 1961), Musoshi (Richards et al., 1988), and Kamoto (Saintilan et al., 2018). This overlaps with the age of the earliest eclogite-facies metamorphism in the CACB (John et al., 2003), suggesting that this mineralization could be the result of crustal re-arrangement during oceanic subduction. However, the mineralization is not preserved within the Lufilian Suture Zone. Instead, this mineralization is perhaps the impact of deglaciation following the Marinoan Snowball Earth event (Saintilan et al., 2018) (Figure 5). Glacial retreat would have resulted in increased erosion of the continent and a resultant renewed influx of metals into the Katangan Basin (Parnell and Boyce, 2019). These metals would have been deposited in a hypersaline, euxinic ocean (Scheller et al., 2018), a setting known to have promoted substantial pyrite deposition (Sansjofre et al., 2016)—ideal conditions for generating metal-rich basinal brines and the deposition of syn-diagenetic copper-sulfide deposits at redox boundaries within the basin.

Finally, the most significant mineralization event in the basin occurred between ~560–470 Ma (Sillitoe et al., 2017). Some studies have argued that this mineralization reflects a metamorphic recrystallisation of syn-diagenetic mineralization during the Lufilian orogeny (e.g., Turlin et al., 2016). However, Sillitoe et al. (2017) argue that the ages reflect a new mineralization event during the Lufilian Orogeny, as molybdenite and copper minerals can withstand amphibolite-grade metamorphism without re-mobilization or isotopic resetting (Sillitoe et al., 2015). Similarly, Torrealday (2000) propose that the mineralized veins in the Kansanshi Cu-Au mine, NW Zambia, are metamorphic in origin. Within the context of the new tectonic framework, these observations point to shortening and crustal thickening during orogenesis as key drivers in the formation of metal deposits, through the development of a thermal and stress regime that enables widespread fluid mobilization. These oxidized metamorphic fluids would have scavenged metals from the orogenic wedge and surrounding sedimentary and basement rocks, precipitating them at redox boundaries. This accounts for the cluster of mineralization events around the time of peak metamorphism at ~530 Ma and potentially throughout the ensuing 10s Myrs during exhumation and cooling. However, it seems clear that syn- to late-orogenic magmatism played a significant role in the formation of metal deposits in the CACB, and provides a more compelling explanation for the concentration of mineralization dated at $\leq$ 510 Myr in particular.

5.1 Evidence for the magmatic origins of CACB mineralization

There are three primary lines of evidence, outlined below, which indicate that magmatism contributed new fluids, metals, and thermal energy to the mineral system of the CACB syn- to post–Lufilian orogeny. It should be noted that this is not without precedent: magmatic-hydrothermal systems overlying granite plutons have been identified as the root of multi-stage REE-Y-Co-Cu-Au sediment-hosted mineralization in the Idaho Cobalt Belt of the Belt-Purcell Basin, USA (Saintilan et al., 2018).

The characteristics of existing deposits Late-stage mineralization, occurring after peak metamorphism, has been associated with high-temperature ($\leq 400\,^{\circ}C$), high-salinity fluids, variably attributed to magmatic sources (El Desouky et al., 2009; Greyling, 2009; Annels, 1989). This interpretation is supported by juvenile osmium isotope signatures in the Kamoto deposit and sulfur isotope data from the Samba deposit, both of which require a magmatic origin (Saintilan et al., 2018; Zhang et al., 2023). Indeed, the brines in the CACB display Cu concentrations overlapping those of magmatic-hydrothermal systems (Davey et al., 2020).

These geochemical signatures align with the known characteristics of several magmatic-related deposits in the region. The Hook Batholith, for instance, hosts iron-oxide-copper-gold (IOCG) deposits (Milani et al., 2019), and the External Fold-Thrust Belt hosts Lufilian-age pegmatites linked to emerald mineralization (Seifert et al., 2004). This belt also contains magmatic-hydrothermal Cu-Au mineralization dated to 530–517 Ma (Perelló et al., 2022), and the Kipushi Mine (Zn-Pb-Cu) in the DRC has been similarly attributed to underlying magmatic activity (Walraven and Chabu, 1994; Heijlen et al., 2008). A magmatic source has also been proposed for cobalt mineralization in the CACB (Annels et al., 1983). Moreover, many CACB deposits exhibit structural and mineralogical features inconsistent with syn-diagenetic or metamorphic models. Instead of standard disseminated textures or small veinlets, deposits such as Kansanshi, Kalengwa, and Safari contain large, cross-cutting, metal-rich veins (Taylor et al., 2013)—often over a metre wide—indicative of a late-stage, high-intensity hydrothermal system.

Temporal correlation between granitic intrusions and mineral deposits Mineralization in the CACB predominantly occurred from ~530–490 Ma, with some deposits as late as 465 Ma (Sillitoe et al., 2017). This time frame overlaps entirely with the intrusion of granites and syenites into the Irumide Belt (534–465 Ma; Johnson et al., 2006), which appears along strike and forms the footwall to the CACB (Figure 1). It also correlates with Lufilian-age alkali-granites/syenites in the Domes Region (Cosi et al., 1992) and granitic pegmatites in the External Fold-Thrust Belt (Seifert et al., 2004). Indeed, the ages of mineralization during the Lufilian appear to show the strongest correlation with magmatism rather than metamorphism or cooling (Figure 3). Based on this timing and structural correlation, it should be expected that late-magmatism would provide a significant control on the mineral system of the CACB.

Localization of distinct metal suites Another striking feature of the CACB is the highly localized distribution of metal suites along strike, and indeed the large variety in metal contents (Cu, Au, Ag, Pb, Ni, Co, etc.) and mineralization styles. For example, the Kansanshi deposit in the Domes Region hosts both copper and gold in a vein-style system, yet gold is entirely absent at the supergiant Cu-only Sentinel mine, located ~100 km along strike. Gold then reappears at the Kasenseli Gold Mine near Mwinilunga, a further ~100 km along strike (data sourced from publicly available mining reports). Even more starkly, the Cu-dominant, Ni-absent Sentinel deposit lies just ~10 km along strike from the Enterprise mine, which hosts abundant hydrothermal nickel but only minor copper mineralization (Capistrant et al., 2015). If such abrupt changes in metal assemblages and mineralization styles were purely sedimentary in origin, it would necessitate a highly segmented basin, with discrete sub-basins on the scale of tens of kilometres, each with a unique metal source. This is an unlikely scenario, particularly given the requirement for high-tonnage, distinct metal sources. An alternative explanation proposed here is that the metals originated from underlying metal-bearing intrusions, with variability in metal assemblages reflecting the spatial distribution and

metal content of these bodies (Darnley, 1960; Gray, 1929). For example, the Zn-Pb-Cu deposit at Kipushi has been attributed to magmatism (see above). Likewise, perhaps the Ni enrichment at the Enterprise deposit reflects input from an underlying syenite and mafic/ultramifc intrusion—potentially a satellite body related to the larger granitoid system responsible for Cu mineralization at Sentinel. Syenites are recognized sources of Ni, as demonstrated in the Scottish Caledonides (Graham et al., 2017), and are commonly spatially associated with ultramafic intrusions, as in Myanmar (Searle et al., 2020).

5.2 Anomalous nature of the CACB mineral system

Ultimately, the anomalous metal endowment of the CACB reflects a combination of factors. First, erosion of a pre-enriched basement would have contributed substantial metal content to the rift-related sedimentary rocks of the Katangan Basin. Second, the prolonged geological evolution of the CACB—from ∼880 Ma to < 500 Ma—allowed ample time for large-scale hydrothermal circulation, metal transport and deposition. Thirdly, the evaporite-rich sedimentary rocks of the Katangan Basin served as a substantial source of sulfur essential for the development of metalliferous basinal brines. Finally, magmatism during and after continent-continent collision introduced a new pulse of heat, metals, and fluids into an already enriched system. As such, the CACB possesses two distinct metal sources: metals derived from the erosion of the basement and those introduced by magmatism during and after continent–continent collision. The metal-rich character of this magmatism is unsurprising, given that the CACB basement previously generated metal-bearing granites during the Mesoproterozoic (Sillitoe et al., 2015).

6 Conclusions

This study reinterprets the Central African Copperbelt (CACB) as a Himalayan-scale, continental-collision orogenic system, characterized by a full Wilson Cycle spanning over 400 million years. The region evolved from continental rifting (∼880 Ma), through ocean basin formation (765–650 Ma), subduction and eclogite-facies metamorphism (650–595 Ma), to continental collision (∼570 Ma), with peak crustal thickening and metamorphism at ∼530 Ma (up to 13 kbar or ∼45 km burial). The new geodynamic model is consistent with structural, petrological, geochronological, and geophysical data, and provides a coherent explanation for the observed regional metamorphism and magmatism—features that are not easily reconciled within the traditional sedimentary-basin framework.

The dominant mineralization event occurred between ∼560–470 Ma, overlapping with peak metamorphism and late-stage thrusting, and temporally coinciding with widespread intrusion of granites and syenites (534–465 Ma). Three lines of evidence support the critical role of magmatism during and after continent-continent collision in metal sourcing, transport and deposition: (1) geochemical and isotopic signatures indicate the presence of hot, high-salinity mineralizing fluids derived from magmatic intrusions; (2) the timing and structural position of mineralization strongly correlates with granite and syenite intrusions across the Domes Region, External Fold-Thrust Belt, and the Irumide Belt; and (3) localized variations in metal assemblages—for example, the Cu-dominant, Ni-absent Sentinel deposit and the nearby Ni-dominant, Cu-poor Enterprise deposit just 10 km apart—strongly suggest that mineralization was controlled by spatially heterogeneous, metal-bearing magmatic intrusions rather than uniform sedimentary processes.

The CACB today hosts some of the world's most significant sediment-hosted deposits—including Kansanshi (1,125.4 Mt

Cu), Sentinel (648.7 Mt Cu), and Konkola ($\geq$140.3 Mt Cu)—and supplies $\sim$14 % of global copper and $\sim$60 % of cobalt. The combination of a pre-enriched basement, evaporite-rich sedimentary sequences, prolonged tectonothermal evolution, and late-stage magmatism accounts for this exceptional endowment. The new geodynamic model establishes a framework for mineral exploration in the CACB and analogous collisional belts worldwide, and indicates that the CACB benefitted from two principal metal sources: metals derived from basement erosion and those introduced by magmatism during and after continent–continent collision. The model predicts that the next generation of metal deposits in the CACB will be found by locating outcropping or shallow subsurface magmatic intrusions.

Acknowledgements

I gratefully acknowledge John-Michael Kendall for funding my post-doctoral research at the University of Oxford. I am indebted to Chris Hawkesworth, Ian Cawood, Peter Cawood, Martin Purkiss, Mike Searle, and Rita Kounoudis for their invaluable comments on earlier drafts of this manuscript. Thanks also to Michael Daly, Laurence Robb, and Tony Watts for engaging discussions on the tectonics of Zambia over the years. I declare no competing interests. All data are available in the manuscript or the supplementary materials.

References (= 100 total)

Annels, A. Ore genesis in the Zambian copperbelt, with particular reference to the northern sector of the Chambishi Basin. *Geological Association of Canada Special Paper*, 36:427 – 452, 1989.

Annels, A., Vaughan, D., and Craig, J. Conditions of ore mineral formation in certain Zambian Copperbelt deposits with special reference to the role of cobalt. *Mineralium Deposita*, 18(1), apr 1983. doi: 10.1007/BF00206696.

Armstrong, R., Master, S., and Robb, L. Geochronology of the Nchanga Granite, and constraints on the maximum age of the Katanga Supergroup, Zambian Copperbelt. *Journal of African Earth Sciences*, 42(1-5):32–40, jul 2005. doi: 10.1016/j.jafrearsci.2005.08.012.

Barron, J. W. *The Stratigraphy, Metamorphism, and Tectonic History of the Solwezi Area, Northwest Province, Zambia: Integrating Geological Field Observations and Airborne Geophysics in the Interpretation of Regional Geology*. PhD thesis, Colorado School of Mines, 2003.

Cahen, L. Review of Geochronological Knowledge in Middle and Northern Africa. *Annals of the New York Academy of Sciences*, 91(2):535–566, 1961. doi: https://doi.org/10.1111/j.1749-6632.1961.tb35519.x.

Cailteux, J., Kampunzu, A., Lerouge, C., Kaputo, A., and Milesi, J. Genesis of sediment-hosted stratiform copper–cobalt deposits, central African Copperbelt. *Journal of African Earth Sciences*, 42(1-5):134–158, July 2005. doi: 10.1016/j.jafrearsci.2005.08.001.

Capistrant, P. L., Hitzman, M. W., Wood, D., Kelly, N. M., Williams, G., Zimba, M., Kuiper, Y., Jack, D., and Stein, H. Geology of the Enterprise Hydrothermal Nickel Deposit, North-Western Province, Zambia. *Economic Geology*, 110(1):9–38, 01 2015. doi: 10.2113/econgeo.110.1.9.

Cawood, P. A. and Buchan, C. Linking accretionary orogenesis with supercontinent assembly. *Earth-Science Reviews*, 82(3):217–256, 2007. doi: https://doi.org/10.1016/j.earscirev.2007.03.003.

Chen, Y., Ye, K., Wu, T. F., and Guo, S. Exhumation of oceanic eclogites: thermodynamic constraints on pressure, temperature, bulk composition and density. *Journal of Metamorphic Geology*, 31(5):549–570, 2013. doi: https://doi.org/10.1111/jmg.12033.

Corfield, R. I. and Searle, M. P. Crustal shortening estimates across the north Indian continental margin, Ladakh, NW India. *Geological Society, London, Special Publications*, 170(1):395–410, 2000. doi: 10.1144/GSL.SP.2000.170.01.21.

Cosi, M., De Bonis, A., Gosso, G., Hunziker, J., Martinotti, G., Moratto, S., Robert, J., and Ruhlman, F. Late proterozoic thrust tectonics, high-pressure metamorphism and uranium mineralization in the Domes Area, Lufilian Arc, Northwestern Zambia. *Precambrian Research*, 58 (1-4):215–240, oct 1992. doi: 10.1016/0301-9268(92)90120-D.

Coward, M. P. and Daly, M. C. Crustal lineaments and shear zones in Africa: Their relationship to plate movements. *Precambrian Research*, 24(1):27–45, feb 1984. doi: 10.1016/0301-9268(84)90068-8.

Cámara, P. and Flinch, J. Chapter 18 - The Southern Pyrenees: A Salt-Based Fold-and-Thrust Belt. In Soto, J. I., Flinch, J. F., and Tari, G., editors, *Permo-Triassic Salt Provinces of Europe, North Africa and the Atlantic Margins*, pages 395–415. Elsevier, 2017. doi: https://doi.org/10.1016/B978-0-12-809417-4.00019-7.

Daly, M. C., Zimba, M., Purkiss, M., and Chibesakunda, F. The Inter-Cratonic Neoproterozoic Katangan Basin of Central Africa: Rift Basin Formation, Orogenic Inversion and Potential Fluid Pathways. *Tectonics*, 44(7):e2025TC008955, 2025. doi: https://doi.org/10.1029/2025TC008955.

Darnley, A. Petrology of some Rhodesian Copperbelt orebodies and associated rocks. *Institute of Mining and Metallurgy Transactions*, 69: 137–173, 1960.

Davey, J., Roberts, S., and Wilkinson, J. J. Copper- and cobalt-rich, ultrapotassic bittern brines responsible for the formation of the Nkana-Mindola deposits, Zambian Copperbelt. *Geology*, 49(3):341–345, 11 2020. doi: 10.1130/G48176.1.

De Swardt, A. M. J., Drysdall, A. R., and Garrard, P. Precambrian geology and structure in central Northern Rhodesia. *Northern Rhodesia,*

geological Survey, Memoir, (2), 1964.

Decrée, S., Étienne Deloule, De Putter, T., Dewaele, S., Mees, F., Yans, J., and Marignac, C. SIMS U–Pb dating of uranium mineralization in the Katanga Copperbelt: Constraints for the geodynamic context. *Ore Geology Reviews*, 40(1):81–89, 2011. doi: https://doi.org/10.1016/j.oregeorev.2011.05.003.

Dirks, P., Kröner, A., Jelsma, H., Sithole, T., and Vinyu, M. Structural relations and Pb-Pb zircon ages for the Makuti gneisses: evidence for a crustal-scale Pan-African shear zone in the Zambezi Belt, northwest Zimbabwe. *Journal of African Earth Sciences*, 28(2):427–442, 1999. doi: https://doi.org/10.1016/S0899-5362(99)00013-5.

Dominish, E., Florin, N., and Teske, S. Responsible Minerals Sourcing for Renewable Energy. Technical report, Institute for Sustainable Futures, University of Technology Sydney., 2019.

Dunkl, I., AntolÍn, B., Wemmer, K., Rantitsch, G., Kienast, M., Montomoli, C., Ding, L., Carosi, R., Appel, E., El Bay, R., Xu, Q., and Von Eynatten, H. Metamorphic evolution of the Tethyan Himalayan flysch in SE Tibet. *Geological Society, London, Special Publications*, 353(1):45–69, jan 2011. doi: 10.1144/SP353.4.

Eglinger, A., André-Mayer, A.-S., Vanderhaeghe, O., Mercadier, J., Cuney, M., Decrée, S., Feybesse, J.-L., and Milesi, J.-P. Geochemical signatures of uranium oxides in the Lufilian belt: From unconformity-related to syn-metamorphic uranium deposits during the Pan-African orogenic cycle. *Ore Geology Reviews*, 54:197–213, 2013. doi: https://doi.org/10.1016/j.oregeorev.2013.04.003.

Eglinger, A., Vanderhaeghe, O., André-Mayer, A. S., Goncalves, P., Zeh, A., Durand, C., and Deloule, E. Tectono-metamorphic evolution of the internal zone of the Pan-African Lufilian orogenic belt (Zambia): Implications for crustal reworking and syn-orogenic uranium mineralizations. *Lithos*, 240-243:167–188, 2016. doi: 10.1016/j.lithos.2015.10.021.

El Desouky, H. A., Muchez, P., and Cailteux, J. Two Cu–Co sulfide phases and contrasting fluid systems in the Katanga Copperbelt, Democratic Republic of Congo. *Ore Geology Reviews*, 36(4):315–332, 2009. doi: https://doi.org/10.1016/j.oregeorev.2009.07.003.

Foster, D. and Goscombe, B. Continental Growth and Recycling in Convergent Orogens with Large Turbidite Fans on Oceanic Crust. *Geosciences*, 3:354–388, 7 2013. doi: 10.3390/geosciences3030354.

Fraser, J. E., Searle, M. P., Parrish, R. R., and Noble, S. R. Chronology of deformation, metamorphism, and magmatism in the southern Karakoram Mountains. *GSA Bulletin*, 113(11):1443–1455, 11 2001. doi: 10.1130/0016-7606(2001)113<1443:CODMAM>2.0.CO;2.

Ghazi, S., Ali, S. H., Sahraeyan, M., and Hanif, T. An overview of tectonosedimentary framework of the Salt Range, northwestern Himalayan fold and thrust belt, Pakistan. *Arabian Journal of Geosciences*, 8:1635–1651, 3 2015. doi: 10.1007/s12517-014-1284-3.

Goscombe, B., Foster, D. A., Gray, D., and Wade, B. Assembly of central Gondwana along the Zambezi Belt: Metamorphic response and basement reactivation during the Kuunga Orogeny. *Gondwana Research*, 80:410–465, 2020. doi: 10.1016/j.gr.2019.11.004.

Graham, S., Holwell, D., McDonald, I., Jenkin, G., Hill, N., Boyce, A., Smith, J., and Sangster, C. Magmatic Cu-Ni-PGE-Au sulfide mineralisation in alkaline igneous systems: An example from the Sron Garbh intrusion, Tyndrum, Scotland. *Ore Geology Reviews*, 80:961–984, 2017. doi: https://doi.org/10.1016/j.oregeorev.2016.08.031.

Gray, A. The outline of the geology and ore deposits of the Nkana concession. In *International Geological Congress*, 1929.

Greyling, L. *Fluid evolution and characterisation of mineralising solutions in the Central African Copperbelt*. PhD Thesis, University of Witwatersrand, Johannesburg, 2009.

Hammarstrom, J. M., Zientek, M. L., Parks, H. L., Dicken, C. L., and U.S. Geological Survey Global Copper Mineral Resource Assessment Team. Assessment of undiscovered copper resources of the world, 2015. Technical report, US Geological Survey, 2019. https://pubs.usgs.gov/publication/sir20185160. ISSN: 2328-0328.

Hanson, R. E., Wilson, T. J., and Wardlaw, M. S. Deformed batholiths in the Pan-African Zambezi belt, Zambia: Age and implications for

regional Proterozoic tectonics. *Geology*, 16(12):1134, 1988. doi: 10.1130/0091-7613(1988)016<1134:DBITPA>2.3.CO;2.

Hanson, R. E., Wardlaw, M. S., Wilson, T. J., and Mwale, G. U-Pb zircon ages from the Hook granite massif and Mwembeshi dislocation: constraints on Pan-African deformation, plutonism, and transcurrent shearing in Central Zambia. *Precambrian Research*, 63(3):189–209, 1993. doi: https://doi.org/10.1016/0301-9268(93)90033-X.

Heijlen, W., Banks, D. A., Muchez, P., Stensgard, B. M., and Yardley, B. W. D. The Nature of Mineralizing Fluids of the Kipushi Zn-Cu Deposit, Katanga, Democratic Repubic of Congo: Quantitative Fluid Inclusion Analysis using Laser Ablation ICP-MS and Bulk Crush-Leach Methods. *Economic Geology*, 103(7):1459–1482, 11 2008. doi: 10.2113/gsecongeo.103.7.1459.

Hitzman, M. and Broughton, D. Discussion:"age of the zambian copperbelt" by sillitoe et al.(2017) mineralium deposita. *Mineralium Deposita*, 52(8):1273–1275, 2017.

Hitzman, M., Kirkham, R., Broughton, D., Thorson, J., and Selley, D. The Sediment-Hosted Stratiform Copper Ore System. In *One Hundredth Anniversary Volume*. Society of Economic Geologists, 2005. doi: 10.5382/AV100.19.

Hoffman, P. F., Abbot, D. S., Ashkenazy, Y., Benn, D. I., Brocks, J. J., Cohen, P. A., Cox, G. M., Creveling, J. R., Donnadieu, Y., Erwin, D. H., Fairchild, I. J., Ferreira, D., Goodman, J. C., Halverson, G. P., Jansen, M. F., Hir, G. L., Love, G. D., Macdonald, F. A., Maloof, A. C., Partin, C. A., Ramstein, G., Rose, B. E. J., Rose, C. V., Sadler, P. M., Tziperman, E., Voigt, A., and Warren, S. G. Snowball Earth climate dynamics and Cryogenian geology-geobiology. *Science Advances*, 3(11):e1600983, 2017. doi: 10.1126/sciadv.1600983.

Hoggard, M. J., Czarnota, K., Richards, F. D., Huston, D. L., Jaques, A. L., and Ghelichkhan, S. Global distribution of sediment-hosted metals controlled by craton edge stability. *Nature Geoscience*, 13(7):504–510, jul 2020. doi: 10.1038/s41561-020-0593-2.

Holwell, D. A., Mitchell, C. L., Howe, G. A., Evans, D. M., Ward, L. A., and Friedman, R. The Munali Ni sulfide deposit, southern Zambia: A multi-stage, mafic-ultramafic, magmatic sulfide-magnetite-apatite-carbonate megabreccia. *Ore Geology Reviews*, 90:553–575, 2017. doi: https://doi.org/10.1016/j.oregeorev.2017.02.034.

Hu, X., Garzanti, E., Wang, J., Huang, W., An, W., and Webb, A. The timing of India-Asia collision onset – Facts, theories, controversies. *Earth-Science Reviews*, 160:264–299, 2016. doi: https://doi.org/10.1016/j.earscirev.2016.07.014.

Jackson, M., Warin, O., Woad, G., and Hudec, M. Neoproterozoic allochthonous salt tectonics during the Lufilian orogeny in the Katangan Copperbelt, central Africa. *Geological Society of America Bulletin - GEOL SOC AMER BULL*, 115:314–330, 03 2003. doi: 10.1130/0016-7606(2003)115<0314:NASTDT>2.0.CO;2.

John, T., Schenk, V., Haase, K., Scherer, E., and Tembo, F. Evidence for a Neoproterozoic ocean in south-central Africa from mid-oceanic-ridge–type geochemical signatures and pressure-temperature estimates of Zambian eclogites. *Geology*, 31(3):243, 2003. doi: 10.1130/0091-7613(2003)031<0243:EFANOI>2.0.CO;2.

John, T., Schenk, V., Mezger, K., and Tembo, F. Timing and PT Evolution of Whiteschist Metamorphism in the Lufilian Arc–Zambezi Belt Orogen (Zambia): Implications for the Assembly of Gondwana. *The Journal of Geology*, 112(1):71–90, jan 2004. doi: 10.1086/379693.

Johnson, S. P., Rivers, T., and Waele, B. D. A review of the Mesoproterozoic to early Palaeozoic magmatic and tectonothermal history of south–central Africa: implications for Rodinia and Gondwana. *Journal of the Geological Society*, 162(3):433–450, 2005. doi: 10.1144/0016-764904-028.

Johnson, S. P., Waele, B. D., and Liyungu, K. A. U-Pb sensitive high-resolution ion microprobe (SHRIMP) zircon geochronology of granitoid rocks in eastern Zambia: Terrane subdivision of the Mesoproterozoic Southern Irumide Belt. *Tectonics*, 25, 12 2006. doi: 10.1029/2006TC001977.

Johnson, S. P., De Waele, B., Evans, D., Banda, W., Tembo, F., Milton, J. A., and Tani, K. Geochronology of the Zambezi supracrustal sequence, southern Zambia: A record of neoproterozoic divergent processes along the southern Margin of the Congo Craton. *Journal of Geology*,

115(3):355–374, 2007. doi: 10.1086/512757.

Kampunzu, A. B., Tembo, F., Matheis, G., Kapenda, D., and Huntsman-Mapila, P. Geochemistry and Tectonic Setting of Mafic Igneous Units in the Neoproterozoic Katangan Basin, Central Africa: Implications for Rodinia Break-up. *Gondwana Research*, 3(2):125–153, 2000. doi: 10.1016/S1342-937X(05)70093-9.

Katongo, C., Koller, F., Kloetzli, U., Koeberl, C., Tembo, F., and Waele, B. D. Petrography, geochemistry, and geochronology of granitoid rocks in the Neoproterozoic-Paleozoic Lufilian–Zambezi belt, Zambia: Implications for tectonic setting and regional correlation. *Journal of African Earth Sciences*, 40(5):219–244, dec 2004. doi: 10.1016/j.jafrearsci.2004.12.007.

Kounoudis, R., Kendall, J. M., Ogden, C. S., Fishwick, S., Chifwepa, C., and Daly, M. C. The tectonic development of the Central African Plateau: evidence from shear-wave splitting. *Geophysical Journal International*, 239(3):1694–1708, oct 2024. doi: 10.1093/gji/ggae345.

Kuribara, Y., Tsunogae, T., Takamura, Y., and Tsutsumi, Y. Petrology, geochemistry, and zircon U-Pb geochronology of the Zambezi Belt in Zimbabwe: Implications for terrane assembly in southern Africa. *Geoscience Frontiers*, 10(6):2021–2044, 2019. doi: https://doi.org/10.1016/j.gsf.2018.05.019.

Lamont, T., McCarthy, W., Strachan, R., Roberts, N., Mackay-Champion, T., Bird, A., and Searle, M. Late Ordovician regional high-pressure metamorphism in Scotland: Caledonian metamorphic climax predated the closure of Iapetus. *EarthArXiv Preprint Server*, 3 2025. doi: 10.31223/X5W13Z.

Master, S. and Ndhlovu, N. M. *Geochemical, Microtextural, and Mineralogical Studies of the Samba Deposit in the Zambian Copperbelt Basement*, chapter 2, pages 37–55. American Geophysical Union (AGU), 2019. doi: https://doi.org/10.1002/9781119290544.ch2.

McCarthy, A., Chelle-Michou, C., Müntener, O., Arculus, R., and Blundy, J. Subduction initiation without magmatism: The case of the missing Alpine magmatic arc. *Geology*, 46(12):1059–1062, 10 2018. doi: 10.1130/G45366.1.

McCuaig, T. C. and Hronsky, J. M. A. The Mineral System Concept: The Key to Exploration Targeting. In *Building Exploration Capability for the 21st Century*. Society of Economic Geologists, 2014. doi: 10.5382/SP.18.08.

Milani, L., Lehmann, J., Naydenov, K. V., Saalmann, K., Kinnaird, J. A., Daly, J. S., Frei, D., and Sanz, A. L.-G. A-type magmatism in a syn-collisional setting: The case of the Pan-African Hook Batholith in Central Zambia. *Lithos*, 216-217:48–72, feb 2015. doi: 10.1016/j.lithos.2014.11.029.

Milani, L., Lehmann, J., Naydenov, K. V., Saalmann, K., Nex, P. A., Kinnaird, J. A., Friedman, I. S., Woolrych, T., and Selley, D. Geology and mineralization of the Cu-rich Mumbwa district, a potential IOCG-type system at the eastern margin of the Pan-African Hook batholith, Zambia. *Journal of African Earth Sciences*, 158:103513, 2019. doi: https://doi.org/10.1016/j.jafrearsci.2019.103513.

Muchez, P., André-Mayer, A.-S., Desouky, H. A. E., and Reisberg, L. Diagenetic origin of the stratiform Cu–Co deposit at Kamoto in the Central African Copperbelt. *Mineralium Deposita*, 50:437–447, 4 2015. doi: 10.1007/s00126-015-0582-3.

Möller, C., Andersson, J., LUNDQVIST, I., and Hellström, F. Linking deformation, migmatite formation and zircon U–Pb geochronology in polymetamorphic orthogneisses, Sveconorwegian Province, Sweden. *Journal of Metamorphic Geology*, 25(7):727–750, 2007. doi: https://doi.org/10.1111/j.1525-1314.2007.00726.x.

Naydenov, K. V., Lehmann, J., Saalmann, K., Milani, L., Kinnaird, J. A., Charlesworth, G., Frei, D., and Rankin, W. New constraints on the Pan-African Orogeny in Central Zambia: A structural and geochronological study of the Hook Batholith and the Mwembeshi Zone. *Tectonophysics*, 637:80–105, 2014. doi: 10.1016/j.tecto.2014.09.010.

Naydenov, K. V., Lehmann, J., Saalmann, K., Milani, L., Poterai, J., Kinnaird, J. A., Charlesworth, G., and Kramers, J. D. The geology of the Matala Dome: an important piece of the Pan-African puzzle in Central Zambia. *International Journal of Earth Sciences*, 105(3):695–712, 2016. doi: 10.1007/s00531-015-1222-y.

O'Brien, P. J. Eclogites and other high-pressure rocks in the Himalaya: a review. *Geological Society, London, Special Publications*, 483(1): 183–213, 2019. doi: 10.1144/SP483.13.

Ogden, C. S., Kounoudis, R., Chifwepa, C., Kendall, M., Holwell, D., Fishwick, S., Nippress, S. E. J., Finch, L., Lane, V., and Daly, M. C. Crustal structure of the Central African Plateau from receiver function analysis. *Geophysical Journal International*, 241(2):1132–1144, 03 2025. doi: 10.1093/gji/ggaf083.

Padilla, A., Otarod, D., Deloach-Overton, S., Kemna, R., Freeman, P., Wolfe, E., Bird, L., Gulley, A., Trippi, M., Dicken, C., Hammarstrom, J., and Brioche, A. Compilation of Geospatial Data (GIS) for the Mineral Industries and Related Infrastructure of Africa. Data release, U.S. Geological Survey, 2021. https://doi.org/10.5066/P97EQWXP.

Pankhurst, R. and Sutherland, D. Caledonian granites and diorites of Scotland and Ireland. 1982.

Parnell, J. and Boyce, A. J. Neoproterozoic copper cycling, and the rise of metazoans. *Scientific Reports*, 9:3638, 3 2019. doi: 10.1038/s41598-019-40484-y.

Perelló, J., Wilson, A., Wilton, J., and Creaser, R. A. Lufilian copper–gold mineralization in the Mkushi District, Zambia: regional metallogenic implications. *Mineralium Deposita*, 57(7):1089–1106, Oct. 2022. doi: 10.1007/s00126-022-01092-5.

Porada, H. and Berhorst, V. Towards a new understanding of the Neoproterozoic-Early Palaeozoic Lufilian and northern Zambezi Belts in Zambia and the Democratic Republic of Congo. *Journal of African Earth Sciences*, 30(3):727–771, 2000. doi: 10.1016/S0899-5362(00)00049-X.

Purkiss, M. Facies and sequence stratigraphy of the Katangan Basin in Zambia. *Journal of African Earth Sciences*, 227:105617, jul 2025. doi: 10.1016/j.jafrearsci.2025.105617.

Rainaud, C., Master, S., Armstrong, R., and Robb, L. Geochronology and nature of the Palaeoproterozoic basement in the Central African Copperbelt (Zambia and the Democratic Republic of Congo), with regional implications. *Journal of African Earth Sciences*, 42(1-5):1–31, jul 2005. doi: 10.1016/j.jafrearsci.2005.08.006.

Richards, J. P., Cumming, G. L., Krstic, D., Wagner, P. A., and Spooner, E. T. C. Pb isotope constraints on the age of sulfide ore deposition and U-Pb age of late uraninite veining at the Musoshi stratiform copper deposit, Central Africa copper belt, Zaire. *Economic Geology*, 83: 724–741, 7 1988. doi: 10.2113/gsecongeo.83.4.724.

Ridgway, J. and Ramsay, C. A provisional metamorphic map of Zambia—explanatory notes. *Journal of African Earth Sciences (1983)*, 5(5): 441–446, 1986.

Saintilan, N. J., Selby, D., Creaser, R. A., and Dewaele, S. Sulphide Re-Os geochronology links orogenesis, salt and Cu-Co ores in the Central African Copperbelt. *Scientific Reports*, 8:14946, 10 2018. doi: 10.1038/s41598-018-33399-7.

Sakuwaha, K. G., Tsunogae, T., Banda, P., Changasha, C., Sikazwe, O. N., and Tsutsumi, Y. Neoproterozoic thermal events and crustal growth in the Zambezi Belt, Zambia: New insights from geothermobarometry, monazite dating, and detrital zircon geochronology of metapelites. *Lithos*, 424-425:106762, 2022. doi: https://doi.org/10.1016/j.lithos.2022.106762.

Sansjofre, P., Cartigny, P., Trindade, R. I., Nogueira, A. C., Agrinier, P., and Ader, M. Multiple sulfur isotope evidence for massive oceanic sulfate depletion in the aftermath of Snowball Earth. *Nature communications*, 7(1):12192, 2016.

Schaeffer, A. J. and Lebedev, S. Global shear speed structure of the upper mantle and transition zone. *Geophysical Journal International*, 194(1):417–449, jul 2013. doi: 10.1093/gji/ggt095.

Scheller, E. L., Dickson, A. J., Canfield, D. E., Korte, C., Kristiansen, K. K., and Dahl, T. W. Ocean redox conditions between the snowballs – Geochemical constraints from Arena Formation, East Greenland. *Precambrian Research*, 319:173–186, 12 2018. doi: 10.1016/j.precamres.2017.12.009.

Searle, M., Cornish, S. B., Heard, A., Charles, J.-H., and Branch, J. Structure of the Northern Moine thrust zone, Loch Eriboll, Scottish Caledonides. *Tectonophysics*, 752:35–51, 2019. doi: https://doi.org/10.1016/j.tecto.2018.12.016.

Searle, M., Garber, J., Hacker, B., Htun, K., Gardiner, N., Waters, D., and Robb, L. Timing of Syenite-Charnockite Magmatism and Ruby and Sapphire Metamorphism in the Mogok Valley Region, Myanmar. *Tectonics*, 39(3):e2019TC005998, 2020. doi: https://doi.org/10.1029/2019TC005998.

Searle, M. P. Tectonic evolution of the Caledonian orogeny in Scotland: a review based on the timing of magmatism, metamorphism and deformation. *Geological Magazine*, 159(1):124–152, 2022. doi: 10.1017/S0016756821000947.

Seifert, A. V., Žáček, V., Vrána, S., Pecina, V., Zachariáš, J., and Zwaan, J. C. Emerald mineralization in the Kafubu area, Zambia. *Bulletin of Geosciences*, 79:1–40, 2004.

Selley, D., Broughton, D., Scott, R., Hitzman, M., Bull, S., Large, R., McGoldrick, P., Croaker, M., Pollington, N., and Barra, F. A New Look at the Geology of the Zambian Copperbelt. In *One Hundredth Anniversary Volume*. Society of Economic Geologists, 2005. doi: 10.5382/AV100.29.

Selley, D., Scott, R., Emsbo, P., Koziy, L., Hitzman, M. W., Bull, S. W., Duffett, M., Sebagenzi, S., Halpin, J., and Broughton, D. W. Structural Configuration of the Central African Copperbelt: Roles of Evaporites in Structural Evolution, Basin Hydrology, and Ore Location. In *Metals, Minerals, and Society*. Society of Economic Geologists, 01 2018. doi: 10.5382/SP.21.07.

Sillitoe, R. H., Perelló, J., Creaser, R. A., Wilton, J., and Dawborn, T. Two Ages of Copper Mineralization in the Mwombezhi Dome, Northwestern Zambia: Metallogenic Implications for the Central African Copperbelt. *Economic Geology*, 110(8):1917–1923, 12 2015. doi: 10.2113/econgeo.110.8.1917.

Sillitoe, R. H., Perelló, J., Creaser, R. A., Wilton, J., Wilson, A. J., and Dawborn, T. Age of the Zambian Copperbelt. *Mineralium Deposita*, 52 (8):1245–1268, dec 2017. doi: 10.1007/s00126-017-0726-8.

Simpson, J. G. The geology of the Mwembeshi River area. Explanation of Degree Sheet 1527, NE Quarter. Technical report, Geological Survey of Zambia, 1962.

St-Onge, M. R., Searle, M. P., and Wodicka, N. Trans-Hudson Orogen of North America and Himalaya-Karakoram-Tibetan Orogen of Asia: Structural and thermal characteristics of the lower and upper plates. *Tectonics*, 25(4), 2006. doi: https://doi.org/10.1029/2005TC001907.

Sun, Z., Lin, J., Qiu, N., Jian, Z., Wang, P., Pang, X., Zheng, J., and Zhu, B. The role of magmatism in the thinning and breakup of the South China Sea continental margin: Special Topic: The South China Sea Ocean Drilling. *National Science Review*, 6(5):871–876, 08 2019. doi: 10.1093/nsr/nwz116.

Taylor, C., Causey, J., Denning, P., Hammarstrom, J., Hayes, T., Horton, J., Kirschbaum, M., Parks, H., Wilson, A., Wintzer, N., and Zientek, M. Descriptive models, grade-tonnage relations, and databases for the assessment of sediment-hosted copper deposits—With emphasis on deposits in the Central African Copperbelt, Democratic Republic of the Congo and Zambia. Scientific Investigations Report 2010–5090–J, U.S. Geological Survey, 2013. http://pubs.usgs.gov/sir/2010/5090/j/. Includes data files.

Torrealday, H. Mineralization and alteration of the Kansanshi copper deposit, Zambia. Master's thesis, Colorado School of Mines, 2000.

Turlin, F., Eglinger, A., Vanderhaeghe, O., André-Mayer, A.-S., Poujol, M., Mercadier, J., and Bartlett, R. Synmetamorphic Cu remobilization during the Pan-African orogeny: Microstructural, petrological and geochronological data on the kyanite-micaschists hosting the Cu(–U) Lumwana deposit in the Western Zambian Copperbelt of the Lufilian belt. *Ore Geology Reviews*, 75:52–75, 2016. doi: https://doi.org/10.1016/j.oregeorev.2015.11.022.

van Gool, J. A. M., Rivers, T., and Calon, T. Grenville Front zone, Gagnon terrane, southwestern Labrador: Configuration of a midcrustal foreland fold-thrust belt. *Tectonics*, 27(1), 2008. doi: https://doi.org/10.1029/2006TC002095.

Villeneuve, M., Gärtner, A., Kalikone, C., and Wazi, N. Amalgamation in the Central African Shield (CAS) by the Kibaran

orogen: New hypothesis and implications for the Rodinia assembly. *Journal of African Earth Sciences*, 202:104936, 2023. doi: https://doi.org/10.1016/j.jafrearsci.2023.104936.

Vrána, S., Prasad, R., and Fediuková, E. Metamorphic kyanite eclogites in the lufilian arc of Zambia. *Contributions to Mineralogy and Petrology*, 51:139–160, 1975. doi: 10.1007/BF00403755.

Walraven, F. and Chabu, M. Pb-isotope constraints on base-metal mineralisation at Kipushi (Southeastern Zaïre). *Journal of African Earth Sciences*, 18(1):73–82, 1994. doi: https://doi.org/10.1016/0899-5362(94)90055-8.

Waters, D. J. Metamorphic constraints on the tectonic evolution of the High Himalaya in Nepal: the art of the possible. *Geological Society, London, Special Publications*, 483(1):325–375, 2019. doi: 10.1144/SP483-2018-187.

Weller, O. M., Mottram, C. M., St-Onge, M. R., Möller, C., Strachan, R., Rivers, T., and Copley, A. The metamorphic and magmatic record of collisional orogens. *Nature Reviews Earth Environment*, 2:781–799, 10 2021. doi: 10.1038/s43017-021-00218-z.

Wendorff, M. Evolution of Neoproterozoic–Lower Palaeozoic Lufilian arc, Central Africa: a new model based on syntectonic conglomerates. *Journal of the Geological Society*, 162(1):5–8, 2005. doi: 10.1144/0016-764904-085.

Yonkee, W. A. and Weil, A. B. Tectonic evolution of the Sevier and Laramide belts within the North American Cordillera orogenic system. *Earth-Science Reviews*, 150:531–593, 2015. doi: https://doi.org/10.1016/j.earscirev.2015.08.001.

Zhang, Y., Zhou, S., Wu, X., and Hu, Q. Genesis of the Samba Cu deposit of the Central African Copperbelt in Zambia: Constraints from geochemistry and geochronology. *GSA Bulletin*, 136(5-6):2343–2358, 10 2023. doi: 10.1130/B37146.1.